Letter

Imbalanced spin coupling in the copper hexamer compounds $A_2Cu_3O(SO_4)_3$ (A_2 = Na$_2$, NaK, K$_2$)

A. Furrer,[1] A. Podlesnyak,[2] E. Pomjakushina,[3] and V. Pomjakushin[1]

[1]*Laboratory for Neutron Scattering, Paul Scherrer Institut, CH-5232 Villigen PSI, Switzerland*

[2]*Neutron Scattering Division, Oak Ridge National Laboratory, Oak Ridge, Tennessee 37831, USA*

[3]*Laboratory for Multiscale Materials Experiments, Paul Scherrer Institut, CH-5232 Villigen PSI, Switzerland*

(Received 28 August 2021; revised 30 October 2021; accepted 17 November 2021; published 2 December 2021)

The minerals $A_2Cu_3O(SO_4)_3$ (A_2 = Na$_2$, NaK, K$_2$) constitute quantum spin systems with copper hexamers as basic structural units. Strong intrahexamer spin couplings give rise to an effective triplet ground state. Weak interhexamer spin couplings are responsible for two-dimensional long-range magnetic order in the (b, c) plane below $3.0 < T_c < 4.7$ K. We investigated the magnetic excitations at $T = 1.5$ K by inelastic neutron scattering (INS). The INS technique was based on the observation of wave vector dependent slices in reciprocal space in order to selectively probe the magnetic signals in different Brillouin zones with different weight. Due to the imbalance of the spin couplings, the data analysis relies on a model in which the interhexamer spin couplings are treated perturbatively on top of the exact $S = 1$ ground state. The interhexamer spin couplings turn out to be ferromagnetic.

DOI: 10.1103/PhysRevB.104.L220401

I. INTRODUCTION

Quantum magnetism and related spin-frustration phenomena are an active field in present condensed-matter research, which has been largely inspired by the discovery of naturally occurring minerals [1]. The minerals $A_2Cu_3O(SO_4)_3$ (A_2 = Na$_2$, NaK, K$_2$) are novel candidates which may advance this field. They are of particular interest, since they are composed of molecularlike copper hexamers with strong intrahexamer and weak interhexamer interactions, so that the interplay of different energy scales and dimensionalities can lead to unusual phenomena. Fujihala *et al.* [2] recognized the fascinating magnetic properties of the title compounds for A_2 = K$_2$, which was proposed to be a one-dimensional antiferromagnet with Cu$_6$ chains along the b direction involving a triplet ground state, giving rise to a novel Haldane system [3] with effective spin $S = 1$ at low temperatures. The $S = 1$ triplet ground state was confirmed by inelastic neutron scattering (INS) experiments performed for the title compounds with A_2 = Na$_2$ and A_2 = K$_2$ [4,5], resulting in detailed values of the intrahexamer exchange parameters J_{nm} marked in Fig. 1 (top) and listed in Table I. The Cu$_6$ chain picture was questioned by Nekrasova *et al.* [6] who proposed two-dimensional antiferromagnetic interactions between the copper hexamers along the diagonals in the (b, c) plane, thereby challenging Fujihala's description of the title compounds in terms of Haldane spin chains. Both Fujihala's and Nekrasova's conclusions, the latter being supported by density functional theory band-structure calculations, are essentially based on magnetic susceptibility, magnetization, and heat capacity data, which constitute integral properties and do not provide reliable information on the magnetic couplings. However, little effort has been made to directly determine the interhexamer exchange parameters j_y and j_z marked in Fig. 1 (top), which are important to discriminate between one-dimensional and two-dimensional magnetic ordering at low temperatures.

INS studies of the dispersive magnetic excitations (spin waves) are usually carried out with use of large enough single crystals, which are not available for the title compounds. Here we demonstrate that a detailed parametrization of the spin waves is possible by using polycrystalline samples. Our method is based on observing wave vector dependent slices in reciprocal space in order to selectively probe the magnetic signals in different Brillouin zones with different weight. The shapes of the observed energy spectra are found to vary substantially by changing the wave vector range, thereby reflecting all the details of the magnetic excitations, so that an unambiguous determination of the interhexamer exchange parameters j_y and j_z becomes possible.

II. SAMPLE CHARACTERIZATION

The compounds $A_2Cu_3O(SO_4)_3$ (A_2 = Na$_2$, K$_2$, NaK) crystallize in the monoclinic space group $C2/c$. Details of the synthesis and characterization of the polycrystalline samples are described in Ref. [4]. The copper hexamers form a two-dimensional magnetic network parallel to the (b, c) plane. The unit cell contains two copper hexamers separated by $\rho = [(1 - 2y)b, c/2]$ as visualized in Fig. 1 (top). The lattice parameters (a, b, c, β) as well as the critical temperatures T_c for magnetic ordering are listed in Table I, and the fractional atomic parameters (x, y, z) are given in Ref. [4] and in the Supplemental Material [7].

III. EXPERIMENTAL RESULTS

The INS experiments were carried out with use of the high-resolution time of flight spectrometer CNCS [8] at the spallation neutron source (SNS) at Oak Ridge National Laboratory. The incoming neutron energy was 3.32 meV,

TABLE I. Lattice parameters a, b, c, β, and unit cell volume V of the compounds $A_2Cu_3O(SO_4)_3$ determined by neutron diffraction at $T = 1.5$ K (Ref. [4] for $A_2 = Na_2$ and $A_2 = K_2$, present work for $A_2 = NaK$). Critical temperature T_c for magnetic ordering [6]. Intrahexamer exchange parameters J_{nm} determined by neutron spectroscopy (Ref. [5] for $A_2 = Na_2$ and $A_2 = K_2$, to be published for $A_2 = NaK$). Parameters Δ, j_y, and j_z of Eq. (3) determined in the present work. The molecular-field parameter is denoted by $2S[J(0) + J'(0)]$.

	$Na_2Cu_3O(SO_4)_3$	$NaKCu_3O(SO_4)_3$	$K_2Cu_3O(SO_4)_3$
a (Å)	17.21406(67)	18.4730(8)	18.97550(66)
b (Å)	9.37286(35)	9.3644(4)	9.50038(35)
c (Å)	14.37014(54)	14.3146(6)	14.19721(51)
β (deg)	111.84364(75)	113.9642(10)	110.49150(85)
V (Å^3)	2152.61	2262.81	2375.66
T_c (K)	3.4	4.7	3.0
J_{11} (meV)	1.3(2)	1.8(2)	1.6(4)
J_{13a} (meV)	–4.7(3)	–4.6(3)	–4.6(3)
J_{13b} (meV)	–8.3(3)	–8.1(3)	–7.9(3)
J_{22} (meV)	2.2(2)	2.9(2)	2.5(3)
J_{23a} (meV)	–5.3(3)	–5.1(3)	–5.2(3)
J_{23b} (meV)	–8.3(3)	–8.1(3)	–7.9(3)
J_{33} (meV)	11.5(1.5)	12.3(1.5)	12.4(1.5)
Δ (meV)	1.22(5)	1.51(3)	1.24(4)
j_y (meV)	0.025(4)	0.050(5)	0.026(3)
j_z (meV)	0.054(4)	0.062(5)	0.056(3)
$2S[J(0) + J'(0)]$ (meV)	1.064	1.392	1.104

yielding an instrumental energy resolution of about 0.1 meV. Figure 2(a) shows the temperature dependence of the energy spectra observed for $A_2 = NaK$. Below $T_c = 4.7$ K there is clear evidence of gapped energy spectra, which extend from 0.8 to 2.0 meV. The wave vector dependence of the energy spectra observed for $A_2 = Na_2$ is shown in Fig. 2(b). The signal above the gap ranges from 0.6 to 1.6 meV. Both the shape and the integrated intensities strongly vary upon changing the modulus of the scattering vector $\mathbf{Q}$. For $A_2 = K_2$ the results are identical within experimental error.

IV. THEORETICAL BACKGROUND

The exchange couplings of the title compounds feature a strong imbalance of the relevant exchange parameters J_{nm} and j_y, j_z, so that the application of the classical spin wave theory turns out to be inadequate. Therefore, our model treats the dominant parameters J_{nm} exactly, providing a triplet ground state with $S = 1$ [4,5]. The additional weak interhexamer interactions j_y and j_z are considered perturbatively to yield the dispersion relations through the Fourier transform of the couplings between the copper hexamers in the (b, c) plane:

$$E(\mathbf{q}) = \Delta - 2S[J(\mathbf{q}) \pm |J'(\mathbf{q})|], \tag{1}$$

where Δ corresponds to the splitting of the ground-state triplet due to the molecular field. The Fourier transforms $J(\mathbf{q})$ and $J'(\mathbf{q})$ of the exchange parameters are given by

$$\begin{aligned} J(\mathbf{q}) &= \sum_{n,m} j_{nm} \exp\{i\mathbf{q} \cdot (\mathbf{R_n} - \mathbf{R_m})\}, \\ J'(\mathbf{q}) &= \sum_{n,k} j_{nk} \exp\{i\mathbf{q} \cdot (\mathbf{R_n} - \mathbf{R_k})\}, \end{aligned} \tag{2}$$

where the summation indices nm and k refer to the copper hexamers in the two sublattices. The parameters j_{nm} and j_{nk} correspond to j_y and j_z, respectively, when the exchange interactions are restricted to nearest-neighbor hexamers as visualized in Fig. 1 (top). The site vectors are $\mathbf{R_n} = (b,0)$ and $\mathbf{R_k} = \boldsymbol{\rho} = [(1\text{-}2y)b, c/2]$. The spin wave dispersion is split into an acoustic and an optic branch associated with the $\pm$ sign in Eq. (1). $J(\mathbf{q})$ is always real, while $J'(\mathbf{q})$ is complex in general. For y we use the value of the center of the Cu_3-Cu_3 bond, which is $y = 0.7475(5)$ for $A_2 = Na_2$, $y = 0.7483(7)$ for $A_2 = NaK$, and $y = 0.7451(7)$ for $A_2 = K_2$ [4,7]. These values are very close to 0.75; thus we set $\boldsymbol{\rho} = [-b/2, c/2]$ and $J'(\mathbf{q})$ becomes real. This is totally justified, since by using the effective y values of the A_2 compounds, we have $|\mathrm{Im}\{J'(\mathbf{q})\}| \ll |\mathrm{Re}\{J'(\mathbf{q})\}|$. In this case the spin wave energies are

$$E(\mathbf{q}) = \Delta - [4j_y \cos(\pi q_y)] \pm 8j_z \cos(\pi q_y/2) \cos(\pi q_z/2)], \tag{3}$$

where $\mathbf{q} = (q_y, q_z)$ with $0 \leqslant q_y, q_z \leqslant 1$. Figure 3 demonstrates the separation into lower-energy acoustic and higher-energy optic spin wave branches. Our model treats the interhexamer couplings j_y and j_z in a phenomenological manner. Microscopically, there are several contributions to both j_y and j_z, but for j_y the dominant couplings are provided by Cu_1-O-S-O-Cu_2 superexchange bridges, whereas for j_z the superexchange bridges Cu_1-O-S-O-Cu_1 and Cu_2-O-S-O-Cu_2 are relevant; see Fig. 1 (top).

The differential neutron cross section for spin waves is given by [9]

$$d^2\sigma/(d\Omega d\omega) \propto S(Q)F^2(\mathbf{Q})[1 \pm \cos(\boldsymbol{\tau} \cdot \boldsymbol{\rho})], \tag{4}$$

where $S(Q)$ is the structure factor of the copper hexamers [5], $F(\mathbf{Q})$ the magnetic form factor, and $\boldsymbol{\tau}$ a reciprocal lattice vector. It follows from Eq. (4) that the Brillouin zones are separated into acoustic and optic zones as visualized in Fig. 1 (bottom).

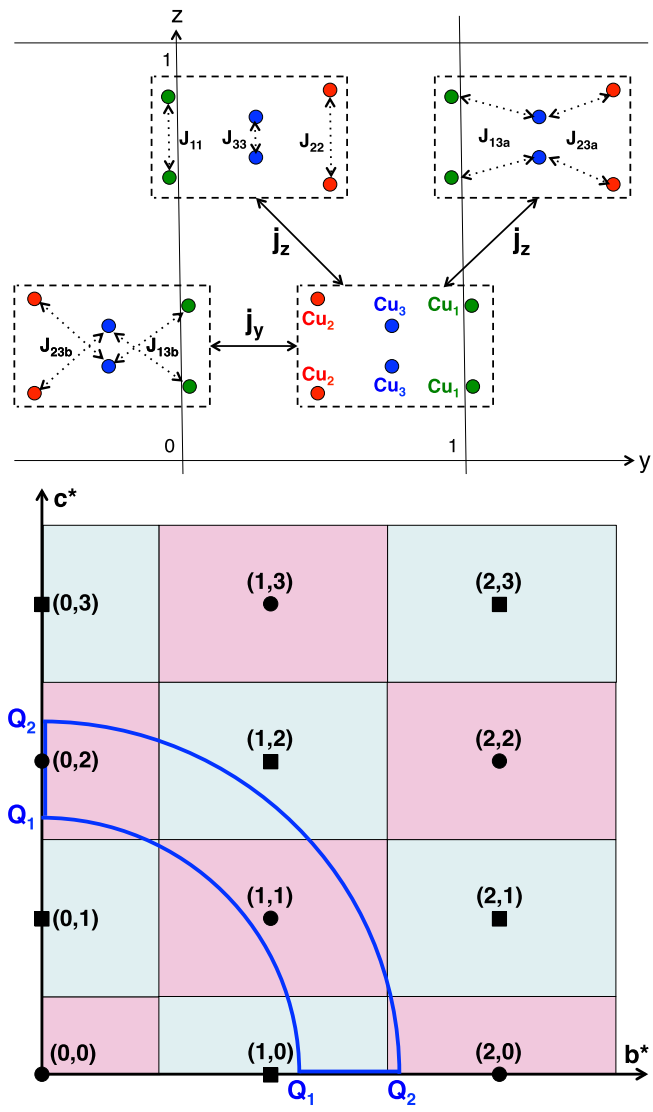

FIG. 1. Top: Projection of the copper hexamers onto the (y, z) plane. The dashed and full arrows mark the relevant intra- and interhexamer exchange parameters J_{nm} and j_y, j_z, respectively. Bottom: Projection of the reciprocal lattice of the A_2 compounds onto the (b^*, c^*) plane. The circles and squares correspond to the centers of the acoustic and optic Brillouin zones shaded in light red and blue colors, respectively. The blue lines define the coverage of the Brillouin zones in neutron scattering experiments for moduli of the scattering vector $\mathbf{Q}$ in the range $Q_1 \leqslant Q \leqslant Q_2$.

V. DATA ANALYSIS

The analysis of the experimental data was based on the detailed Q dependence of the energy spectra shown in Fig. 4. The data for $A_2 = \mathrm{Na_2}$ are very similar to those for $A_2 = \mathrm{K_2}$. The integrated intensities nicely follow the sinusoidal Q dependence according to the structure factor $S(Q)$ for transitions within the ground-state triplet; see Eq. (4). The variation of the range $Q_1 \leqslant Q \leqslant Q_2$ strongly changes the coverage C of the acoustic (A) and optic (O) Brillouin zones. From bottom to top in Fig. 4 we have $C_\mathrm{A}/C_\mathrm{O} = 1.78,\ 0.72,\ 1.08$, and 1.28, which is directly reflected by the Q dependence of the intensities associated with acoustic Brillouin zones in the lower-energy part of the spectra.

A rough estimate of the spin wave parameters is obtained from selected points in reciprocal space, which can be used as starting parameters in the least-squares fitting procedures. The energies defined by Eq. (3) for $\mathbf{q} = (0,0)$ determine the lower and upper limit of the observed energy spectra:

$$\mathbf{q} = (0,0):\ E_\mathrm{acoustic}(\mathbf{q}) = \Delta - 4j_y - 8j_z,$$
$$E_\mathrm{optic}(\mathbf{q}) = \Delta - 4j_y + 8j_z,$$

which essentially fixes the value of j_z. Large contributions to the energy spectra are expected around the $\mathbf{q}$ vectors where the derivative $dE(\mathbf{q})/d\mathbf{q} = 0$. This is the case for $\mathbf{q} = (0,0)$ as well as for

$$\mathbf{q} = (1,1):\ E_\mathrm{acoustic}(\mathbf{q}) = E_\mathrm{optic}(\mathbf{q}) = \Delta + 4j_y;$$

see Fig. 3. The energy spectra observed for $A_2 = \mathrm{NaK}$ are considerably different from $A_2 = \mathrm{K_2}$ and $A_2 = \mathrm{Na_2}$ concerning both the energy range and the spectral shape, the latter being due to the small dispersion of the optic spin wave branches along the (1,0) and (1,1) directions which results in enhanced intensities at the upper energy limit.

Δ, j_y, and j_z were treated as adjustable parameters in the least-squares fitting analysis of the data displayed in Fig. 4. For each wave vector range $Q_1 \leqslant Q \leqslant Q_2$, the spin wave energies were collected in pixels of size 0.002×0.002 Å^{-2} and folded with the instrumental energy resolution. The results are listed in Table I and shown in Figs. 3 and 4. Good agreement between the experimental and calculated energy spectra is obtained with overall standard deviations $\chi^2 = 1.9$ and $\chi^2 = 3.0$ for $A_2 = \mathrm{K_2}$ and $A_2 = \mathrm{NaK}$, respectively. Both exchange parameters j_y and j_z turn out to be ferromagnetic; any attempts to reproduce the observed energy spectra with antiferromagnetic and mixed ferromagnetic/antiferromagnetic exchange parameters failed as demonstrated in detail in Ref. [7].

In principle, there is a self-consistent criterion relating the gap parameter Δ to the Fourier transform of the exchange parameters:

$$\Delta = 2S[J(0) + J'(0)] = 4j_y + 8j_z. \tag{5}$$

As shown in Table I, the calculated values for $2S[J(0) + J'(0)]$ are slightly smaller than Δ. The difference is probably due to a gap enhancement D resulting from the single-molecule axial anisotropy, which was suggested to be present for the copper hexamers with $D = 0.064$ meV (for $A_2 = \mathrm{Na_2}$ and $A_2 = \mathrm{K_2}$) and $D = 0.079$ meV (for $A_2 = \mathrm{NaK}$) [6]. The molecular-field parameter $2S[J(0) + J'(0)]$ for $A_2 = \mathrm{NaK}$ is larger than for $A_2 = \mathrm{Na_2}$ and $A_2 = \mathrm{K_2}$, which explains the difference of the critical temperatures T_c for long-range magnetic order; see Table I.

VI. CONCLUDING REMARKS

The results of the present work are in strong contradiction to earlier findings reported in Refs. [2,6]. Our analysis gives compelling evidence for superexchange interhexamer couplings both along the b axis and along the diagonals in the (b, c) plane, and the corresponding exchange parameters j_y and j_z are ferromagnetic. This implies that the two-dimensional magnetic structure of the A_2 compounds

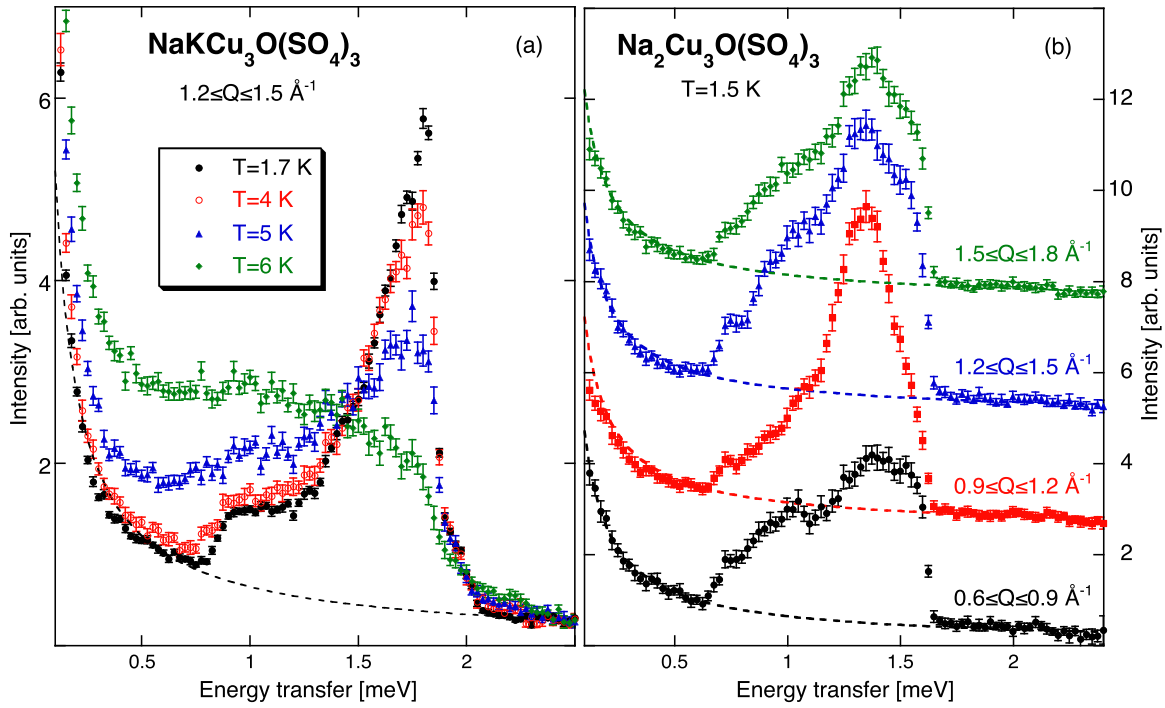

FIG. 2. (a) Temperature dependence of the energy spectra observed for $NaKCu_3O(SO_4)_3$. The dashed curve corresponds to a power law describing the tail of the elastic line. (b) Wave vector dependence of the energy spectra observed for $Na_2Cu_3O(SO_4)_3$ at $T = 1.5$ K. The dashed curves are as in (a). For clarity, the data of the upper three spectra are enhanced by 2.5, 5, and 7.5 intensity units.

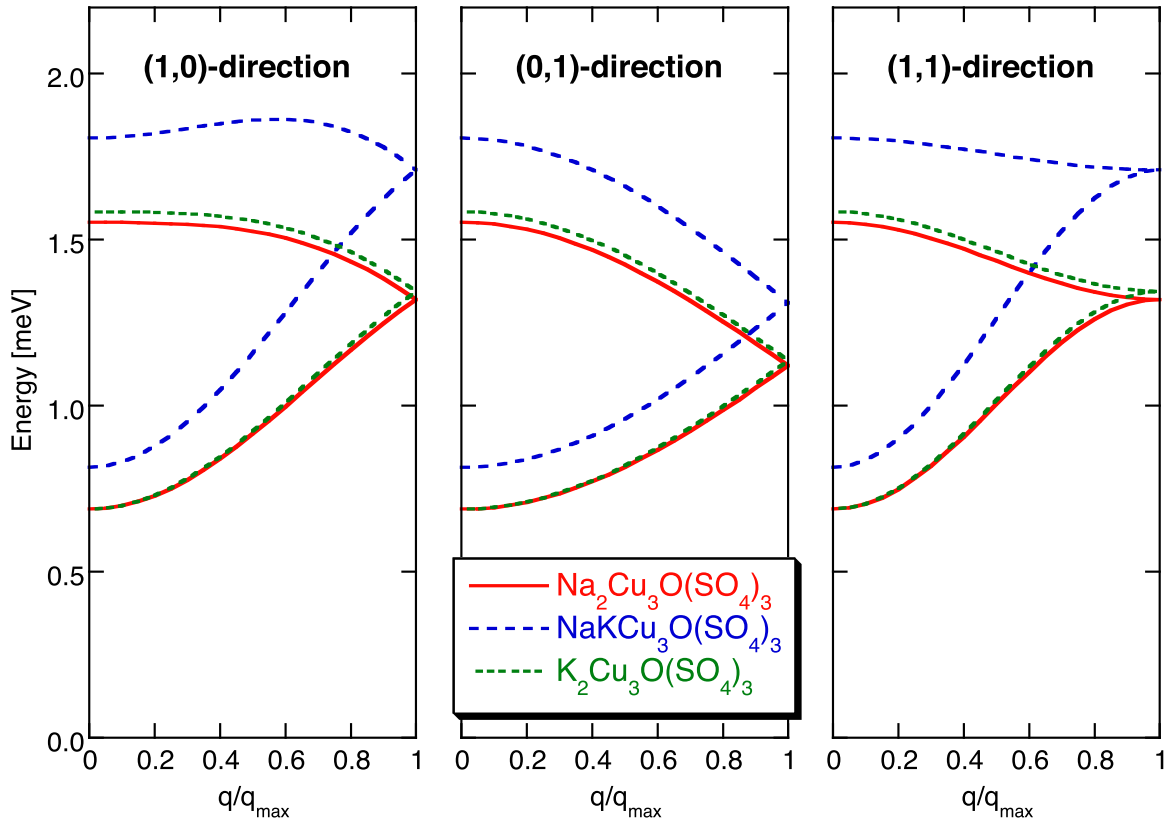

FIG. 3. Spin wave dispersions of the A_2 compounds along the three symmetry directions in the (b^*, c^*) plane.

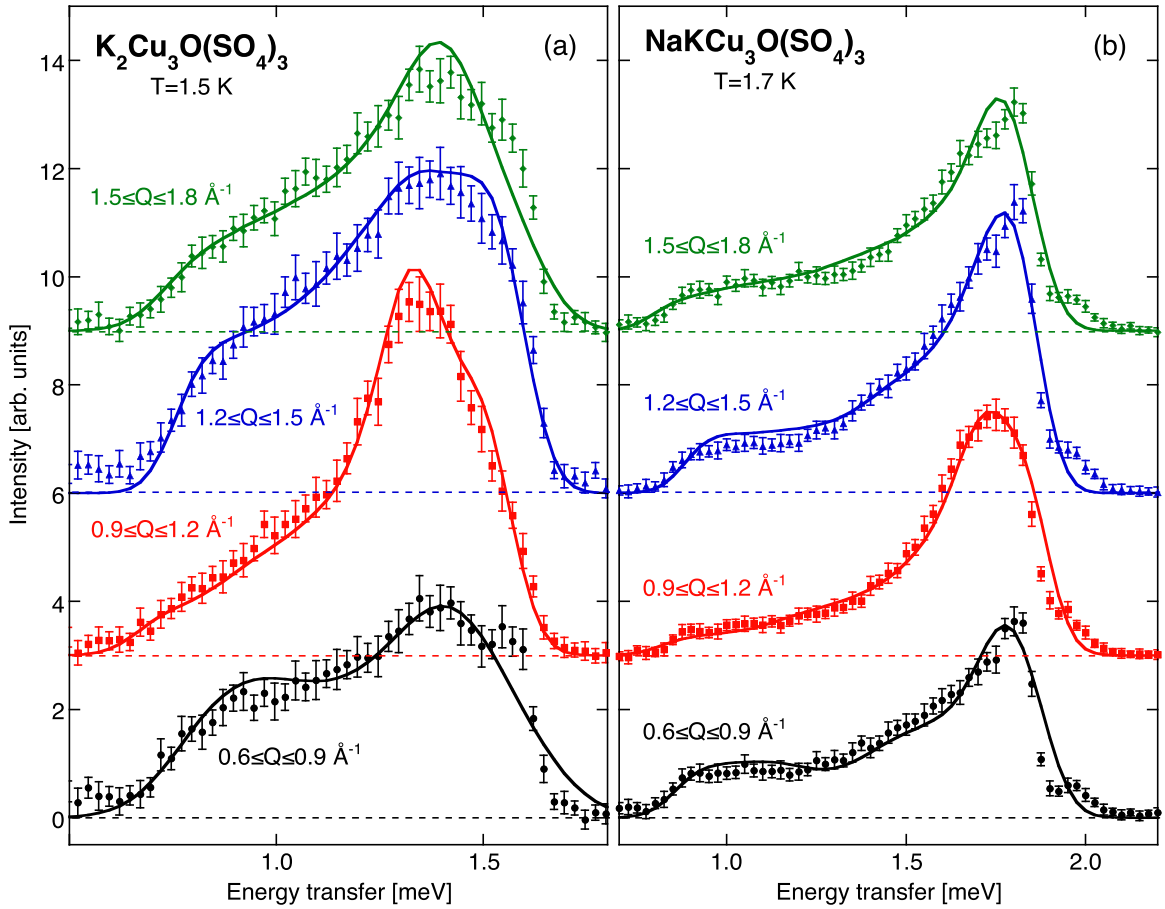

FIG. 4. Energy spectra observed for $A_2Cu_3O(SO_4)_3$ with $A_2 = K_2$ (a) and $A_2 = NaK$ (b). A power-law background is subtracted from the experimental data (see Fig. 2). The lines correspond to least-squares fits based on Eqs. (3) and (4). For clarity, the data of the upper three spectra are enhanced by 3, 6, and 9 intensity units.

should reflect their basically ferromagnetic nature. Studies along these lines have been presented by Hase *et al.* [10] based on neutron diffraction experiments performed for $A_2 = K_2$ at low temperatures, indicating the presence of two-dimensional magnetic order with propagation vector $\mathbf{k} = (0, 0, 0)$ and ferromagnetic spin alignments along the b axis.

The compounds $A_2Cu_3O(SO_4)_3$ constitute a rare example of isostructural systems for which the physical properties of the mixed compound $A_2 = NaK$ cannot be interpolated between the pure compounds $A_2 = Na_2$ and $A_2 = K_2$ This is evident, e.g., for the lattice parameters b as well as for the magnetic ordering temperatures T_c which for $A_2 = NaK$ lie outside the limits given by the pure compounds; see Table I. The anomalously low value of b has an effect on the interhexamer coupling parameter j_y which turns out to be twice as large compared to $A_2 = Na_2$ and $A_2 = K_2$, whereas the coupling parameters j_z are very similar for all A_2 compounds.

In conclusion, our work demonstrates that a reliable determination of spin-coupling parameters requires the use of direct methods such as INS spectroscopy. This is particularly true for magnetic compounds with unbalanced and frustrated spin interactions, where *ab initio* calculations have to be considered with caution. We introduced an experimental technique to analyze INS data taken for polycrystalline samples, which will be a very useful alternative in cases where single crystals are not available.

ACKNOWLEDGMENTS

Part of this work was performed at the Swiss Spallation Neutron Source (SINQ), Paul Scherrer Institut (PSI), Villigen, Switzerland. This research used resources at the Spallation Neutron Source, a DOE Office of Science User Facility operated by the Oak Ridge National Laboratory.

[1] D. S. Inosov, Adv. Phys. **67**, 149 (2018).
[2] M. Fujihala, T. Sugimoto, T. Tohyama, S. Mitsuda, R. A. Mole, D. H. Yu, S. Yano, Y. Inagaki, H. Morodomi, T. Kawae, H. Sagayama, R. Kumai, Y. Murakami, K. Tomiyasu, A. Matsuo, and K. Kindo, Phys. Rev. Lett. **120**, 077201 (2018).
[3] F. D. M. Haldane, Phys. Rev. Lett. **50**, 1153 (1983).
[4] A. Furrer, A. Podlesnyak, E. Pomjakushina, and V. Pomjakushin, Phys. Rev. B **98**, 180410(R) (2018).
[5] A. Furrer, A. Podlesnyak, J. M. Clemente-Juan, E. Pomjakushina, and H. U. Güdel, Phys. Rev. B **101**, 224417 (2020).
[6] D. O. Nekrasova, A. A. Tsirlin, M. Colmont, O. Siidra, H. Vezin, and O. Mentré, Phys. Rev. B **102**, 184405 (2020).
[7] See Supplemental Material at http://link.aps.org/supplemental/10.1103/PhysRevB.104.L220401 for neutron diffraction results and analysis of the observed energy spectra.
[8] G. Ehlers, A. A. Podlesnyak, J. L. Niedziela, E. B. Iverson, and P. E. Sokol, Rev. Sci. Instrum. **82**, 085108 (2011).
[9] A. Furrer, J. Mesot, and T. Strässle, in *Neutron Scattering in Condensed Matter Physics* (World Scientific, Singapore, 2009).
[10] M. Hase, K. C. Rule, J. R. Hester, J. A. Fernandez-Baca, T. Masuda, and Y. Matsuo, J. Phys. Soc. Jpn. **88**, 094708 (2019).